Liquid Crystals
Publication details, including instructions for authors and subscription information:
http://www.informaworld.com/smpp/title~content=t713926090

Wave mixing in electric field biased nematic thin films

Shu-Hsia Chen[a]; Tien-Jung Chen[a]; Yuhren Shen[a]; Chen-Lung Kuo[a]
[a] Institute of Electro-Optical Engineering, National Chiao Tung University, Taiwan, Republic of China

To cite this Article Chen, Shu-Hsia , Chen, Tien-Jung , Shen, Yuhren and Kuo, Chen-Lung(1993) 'Wave mixing in electric field biased nematic thin films', Liquid Crystals, 14: 1, 185 — 196
To link to this Article: DOI: 10.1080/02678299308027311
URL: http://dx.doi.org/10.1080/02678299308027311

LIQUID CRYSTALS, 1993, VOL. 14, NO. 1, 185–196

Invited Lecture

Wave mixing in electric field biased nematic thin films

by SHU-HSIA CHEN*, TIEN-JUNG CHEN, YUHREN SHEN and CHEN-LUNG KUO

Institute of Electro-Optical Engineering, National Chiao Tung University, Hsinchu, Taiwan 300, Republic of China

Wave mixing due to molecular reorientation in electric field biased nematic thin films is studied. By using the continuum theory, general formulae have been derived for the orientational angle distribution. The concept of a thin film grating is utilized to describe the diffraction efficiency. Experimental results which exhibit the behaviours of the transmission beam and diffraction beams have been obtained as predicted by the numerical calculation.

1. Introduction

The non-linear optical phenomena associated with two input laser beams superimposed on a liquid crystal film can be understood by the picture of material excitation [1]. There exists, in general, a large variety of possible material excitations in a medium. For liquid crystals, the molecular reorientation is a special and important material excitation. In the degenerate optical mixing case, two input beams having the same frequency can create a static grating, whereas the material excitations at zero frequency lead to a static refractive index variation. Thus, the static grating corresponds to a refractive index grating. The output beam of the wave mixing process is then the result of diffraction of the input wave from this grating.

For the nematic liquid crystal (NLC), the local molecular reorientation can be found by continuum theory. The non-linear coupling coefficient in the coupled-wave equations, which are usually used to describe the non-linear wave mixing process [1, 2], is not a constant for this two input beam system. It depends not only on material parameters but also on the experimental geometry, i.e. the distorted NLC structure. The one elastic constant model disregarding the twist deformation for this system was worked out in 1979 by Herman *et al.* [3] with a biased magnetic field. Obviously a biased external field, which can induce molecular reorientation, plays an important role in non-linear optical phenomena in liquid crystals. We presented a general theoretical model for this system with a homeotropically aligned NLC including a biased low frequency electric field and considered the twist effects [4]. The nearly normally incident laser beams have a polarization perpendicular to their incident plane. For the first order non-linear optical diffraction, we found that there is a peak diffraction efficiency, instead of a monotonic decrease, with respect to the biased field.

In the meantime, the large peak shift from the Frédericksz threshold value and the suppression of diffraction were obtained by experiment and calculation. We found that peaks of the same efficiency can be observed at two distinct voltages if the phase amplitude of the induced grating is large enough. The crucial factor accounting for these phenomena was the difference in the bend and the splay elastic constants in addition to

* Author for correspondence.

0267–8292/93 $10·00

the twist deformation [5–7]. The behaviour of the wave mixing was characterized not only by the intrinsic properties of the NLC material but also by the experimental parameters. The optimal reduced effective field for diffraction efficiency depends on the input optical intensity, the grating period, the elastic constants and the sample thickness d [8].

Actually, multiple order diffractions can occur in this system when the exciting laser intensity is high. Weak beam amplification can be observed when the input intensity difference is large. In this paper we present the behaviour of the high order diffraction and weak beam amplification for this system.

In this paper, the general theory reported in [4] is reviewed and extended to include both homeotropic and planar samples. The diffraction efficiency is derived for every order. A formula for the gain is shown. The behaviour of the diffraction efficiency with respect to the biased electric field is illustrated both numerically and experimentally. The gain for weak beam amplification with respect to the biased electric field, and the input laser intensity are studied.

2. Theory

The basic theory is essentially the same for homeotropic and planar cells. Therefore we consider the homeotropic cell first, then change the formulation to include a planar cell. The geometry shown in figure 1 is used. Two linearly polarized laser beams, having a small crossing angle α, are nearly normally incident on the cell with the incident plane coinciding with the XZ plane. The light polarization lies in the Y direction. The easy directions of the homeotropic and planar cell are in the Z and Y directions, respectively. For a sufficiently thin liquid crystal film, degenerate wave mixing can be simply described by diffraction from an induced phase grating. The picture is that the interference of two linearly polarized laser beams with intensity I_1 and I_2, respectively,

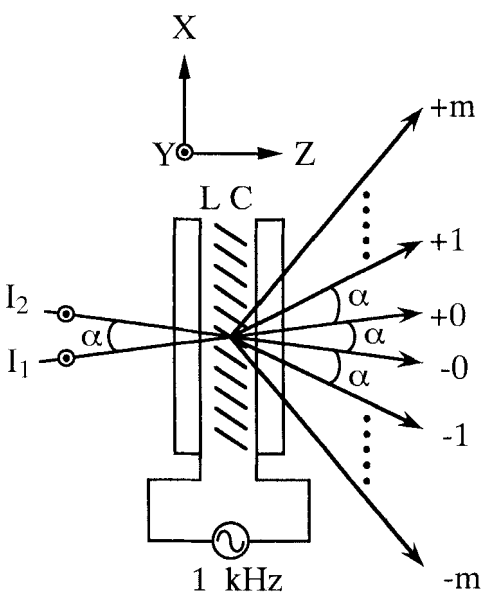

Figure 1. Schematic diagram of degenerate wave mixing with two input beams in an electric field biased nematic film.

produces a sinusoidally varying intensity pattern, $I = I_1 + I_2 + 2\sqrt{(I_1 I_2)}\cos(2\pi X/\Lambda)$, in the cell with a period Λ. The optical fields superpose on the applied electric field and create a periodically distorted molecular-reorientation structure, which then gives rise to an induced phase grating with the same period. This phase grating diffracts the original incident beams on both sides.

For a homeotropically aligned nematic liquid crystal cell, the free energy density F can be written as the following:

$$F = \frac{1}{2}\left[K_2\left(\frac{\partial\theta}{\partial X}\right)^2 + K_3(1 - K\sin^2\theta)\left(\frac{\partial\theta}{\partial Z}\right)^2\right] - \frac{D_z^2}{8\pi\varepsilon_{\|}}\frac{1}{1 - w\sin^2\theta} - \frac{I}{C}\frac{n_o}{\sqrt{(1 - u\sin^2\theta)}}, \tag{1}$$

where $K \equiv 1 - K_1/K_3$, $u = 1 - n_o^2/n_e^2$, $w = 1 - \varepsilon_{\perp}/\varepsilon_{\|}$, K_1, K_2, and K_3 represent the splay, twist and bend elastic constants, respectively, D_z is the Z component of the electric displacement, I is the optical intensity and C is the velocity of light in a vacuum. We use a trial solution for the reorientational angle of local average,

$$\theta(X, Z) = [\theta_1 + \theta_2\cos(2\pi X/\Lambda)]\sin(\pi Z/d),$$

with the boundary condition, $\theta(Z = 0) = \theta(Z = d) = 0$. Here θ_1 and θ_2 represent the transverse spatial average of the orientational angle and the amplitude of the modulation, respectively. The equilibrium values of the constants θ_1 and θ_2 can be calculated from the minimization of the total free energy, $F = \int F\,dV$, by letting $\partial F/\partial\theta_1 = 0$ and $\partial F/\partial\theta_2 = 0$, we then have

$$\theta_1 - KG_1(\theta_1, \theta_2) - (V/V_{th})^2 G_2(\theta_1, \theta_2) - I_r G_3(\theta_1, \theta_2) + (I_t/I_{th})G_4(\theta_1, \theta_2) = 0, \tag{2}$$

and

$$\theta_2[1 + 2a - KG_5(\theta_1, \theta_2)] - 2I_r J_1(2\theta_1) - [(I_t/I_{th}) + (V/V_{th})^2]G_3(\theta_1, \theta_2) = 0, \tag{3}$$

where the functions $G_i(\theta_1, \theta_2)$ are the same as those stated in [4], $a \equiv 2(K_2/K_3)(d/\Lambda)^2$ is termed the twist ratio, $V_{th} = \pi\sqrt{(4\pi K_3/|\Delta\varepsilon|)}$ is the threshold voltage with $\Delta\varepsilon = \varepsilon_{\|} - \varepsilon_{\perp}$, $I_{th} = (\pi/d)^2(CK_3/n_o|u|)$ is the threshold intensity, $I_r = \sqrt{(I_1 I_2)}/I_{th}$ and $I_t = I_1 + I_2$, $J_i(2\theta_1)$ is the Bessel function of first kind of order i. With $\theta_2^2 \ll 1$, a more explicit form of θ_2 can be obtained as

$$\theta_2 \cong \frac{2I_r J_1(2\theta_1)}{1 + (K_2/K_3)(2d/\Lambda)^2 - [b + 1][J_0(2\theta_1) - J_2(2\theta_1)] - KG_5(\theta_1, 0)}, \tag{4}$$

where $b \equiv I_t/I_{th} + (V/V_{th})^2 - 1$ is the reduced effective field.

The effective refractive index $n(X)$ is

$$n(X) = \bar{n} + \Delta\bar{n}_{NL}\cos\left(\frac{2\pi X}{\Lambda}\right), \tag{5}$$

where $\bar{n} = n_o + |u|n_o[1 - J_0(2\theta_1)]/4$ is the spatially uniform refractive index and $\Delta\bar{n}_{NL} = |u|n_o\theta_2 J_1(2\theta_1)/2$ is the modulation index of the grating. For a Kerr medium, the refractive index change is proportional to the pump intensity, i.e. $\Delta\bar{n}_{NL} = \bar{n}_2\sqrt{(I_1 I_2)}$, where $\bar{n}_2$ is the Kerr coefficient.

The corresponding induced phase shift of the probing beam across the sample is

$$\delta(X) = \delta_0 + \delta_1\cos\left(\frac{2\pi X}{\Lambda}\right), \tag{6}$$

where $\delta_0 = \bar{n}(2\pi/\lambda_0)d$ and $\delta_1 = \Delta\bar{n}_{NL}(2\pi/\lambda_0)d$ are the spatial average phase retardation and the modulation amplitude of the phase grating, respectively.

The diffraction efficiency for two input beams with intensities I_1 and I_2, defined as the ratio of the diffraction intensity I_{Dm} to the total incident intensity I_t, is derived as

$$\eta_m = \frac{I_{Dm}}{I_t} = r_1 J_m^2(\delta_1) + r_2 J_{m+1}^2(\delta_1), \tag{7}$$

and

$$\eta_{-m} = \frac{I_{-Dm}}{I_t} = r_1 J_{m+1}^2(\delta_1) + r_2 J_m^2(\delta_1), \quad m = 0, 1, 2, \ldots, \tag{8}$$

where $r_1 = I_1/I_t$, $r_2 = I_2/I_t$ and I_{+D0}, I_{-D0} are the intensities of the transmitted beams of I_1 and I_2, respectively.

To illustrate the peculiar behaviour of the diffraction efficiency and the transmitted intensity, two cases are emphasized. One, with two input beams of equal intensity, shows high order diffraction behaviour. The other, with two input beams of different intensity, exhibits weak beam amplification.

For a NLC cell with $I_1 = I_2$, we obtain $r_1 = r_2$ and $\eta_m = \eta_{-m}$ in equations (7) and (8). The behaviour of the diffraction efficiency is characterized by the properties of the Bessel function $J_i(\delta_1)$ and the amplitude of the phase modulation δ_1. The lower orders of η_m with respect to δ_1 are plotted in figure 2. It is obvious that there is more than one local maximum, or diffraction peak, with respect to the amplitude δ_1. However, δ_1 is in reality limited by the experimental parameters. For example, in the situation of the external field biased film, the phase amplitude δ_1 has a local maximum δ_{1m} instead of monotonically increasing with respect to the reduced effective field b [4]. Let η_{mn} and ϕ_{mn} denote the diffraction efficiency and phase amplitude of the nth peak of mth order diffraction, respectively, in figure 2. To observe the behaviour of η_m with respect to b, let us assume δ_{1m} to be 4 rad which is smaller than ϕ_{31} but greater than ϕ_{21}. In other words, δ_1 increases to approach δ_{1m} then decreases with the increment of b. In the mean

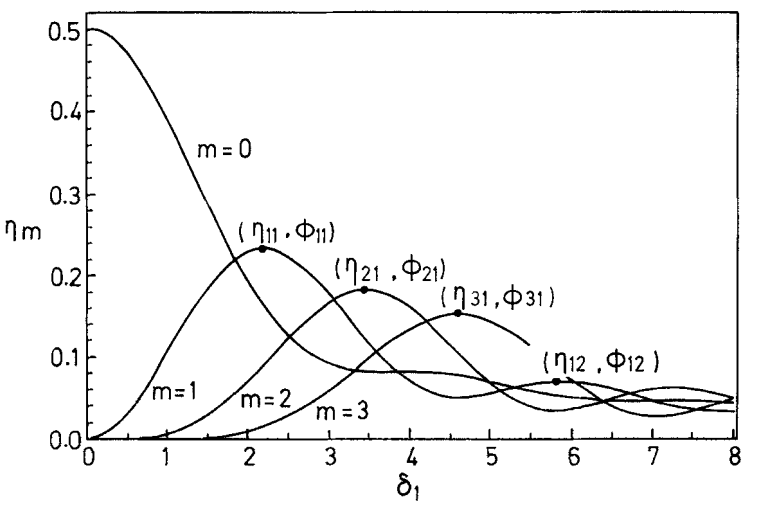

Figure 2. Numerical results of the diffraction efficiency η_m versus the modulation amplitude of the phase grating δ_1.

time, η_1 exhibits double peaks with the same maximum efficiency, η_{11}, at $\delta_1 = \phi_{11}$ but at two distinct values of b. Similarly, the second order diffraction exhibits double peaks with respect to b also. However, for the third order diffraction, there is only one diffraction peak with respect to b since $\phi_{31} > 4$ and the maximum efficiency has a value of $\eta_3(4)$.

For weak beam amplification, the gain is defined as the intensity ratio of the transmitted beam I_{D0} to the weak input beam I_{wk}, that is

$$g = \frac{I_{D0}}{I_{wk}} = J_0^2(\delta_1) + \frac{I_{st}}{I_{wk}} J_1^2(\delta_1), \tag{9}$$

where I_{st} is the intensity of the strong input beam. To see the relation of the gain to the intrinsic properties of the liquid crystal and the experimental parameters, the analytical solution is obtained under the assumption $\theta_2^2 \ll \theta_1^2 \ll 1$. That is

$$g \approx 1 + \frac{C_0^2 I_{st}[I_{st} - 2I_{wk}]}{I_{th}^2} \frac{b^2(1-2b)^2}{(a+b)(1-K)^3}, \tag{10}$$

where $C_0 = \pi |u| n_o d/\lambda_0$.

We can easily see from the above equation that the gain is greater than one if $I_{st} > 2I_{wk}$, and we have weak beam amplification. In the meantime, for a given I_{st}, the gain increases to a saturating value as the beam ratio, I_{st}/I_{wk}, increases. Keeping the beam ratio constant, the gain increases monotonically with respect to the total input intensity.

All the above equations are valid for a planar cell if we exchange K_3, $\varepsilon_{\|}$ and n_e with K_1, $\varepsilon_{\perp}$ and n_o, respectively, and use $b = (V/V_{th})^2 - (I_t/I_{th}) - 1$ for the reduced effective field.

3. Numerical results

The argument for the behaviour of the diffraction peaks in the last section is verified by numerical calculation. Using equations (2), (4), (5), (6) and (7), the diffraction efficiencies of the lowest three orders have been calculated for a homeotropically aligned MBBA cell. The material parameters used are $n_e = 1{\cdot}81$, $n_o = 1{\cdot}57$, $\Delta\varepsilon = -0{\cdot}7$, $K_1 = 5{\cdot}8 \times 10^{-7}$ dyne, $K_2 = 4 \times 10^{-7}$ dyne and $K_3 = 7{\cdot}5 \times 10^{-7}$ dyne. Three different input intensities are used and those are 16·3 W cm^{-2}, 22·9 W cm^{-2} and 28·2 W cm^{-2}. Other parameters, $\Lambda = 0{\cdot}12$ mm, $\lambda_0 = 514{\cdot}5$ μm, $d = 100$ μm, $V_{th} = 3{\cdot}458$ V and $I_{th} = 571{\cdot}26$ W cm^{-2} are used in all three calculations.

The numerical results for the lowest input intensity are shown in figure 3 (*a*). There is a single peak for each diffraction order. This indicates that the maximum phase amplitude δ_{1m} is less than ϕ_{11} in figure 2. The peaks occur at the same b value. As the input intensity increases, the first order diffraction has double peaks as shown in figure 4 (*a*). However, the second and third order diffractions both have a single peak. The maximum phase amplitude is greater than ϕ_{11} but less than ϕ_{21}. The local minimum of the first order diffraction and the peaks of second and third orders are at the same reduced effective field b. The diffraction efficiencies of the double peaks are the same and equal to η_{11}. For the largest input intensity, both first and second orders have double peaks as shown in figure 5 (*a*). The local minima of the first and second order diffraction efficiencies and the peak of third order are at the same b as predicted by figure 2. The maximum phase amplitude therefore must be greater than ϕ_{21} and less than ϕ_{31}.

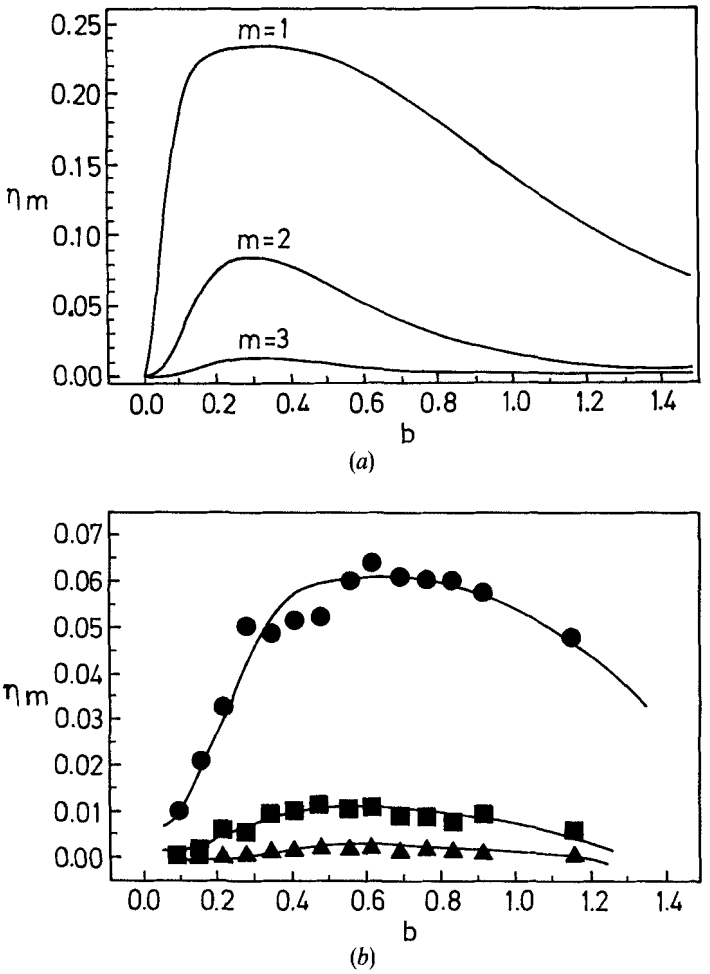

Figure 3. Numerical results (*a*) and experimental results (*b*) of the diffraction efficiency η_m versus the reduced effective field b, for $I_1 = I_2$, shows $\delta_{1m} < \phi_{11}$. The solid lines plotted in (*b*) are a guide to the eyes. (*a*) $I_t/I_{th} = 0{\cdot}057$; (*b*) $I_t/I_{th} = 0{\cdot}057$; ●, $m=1$; ■, $m=2$; ▲, $m=3$.

For the weak beam amplification, the scattering loss is considered for the interacting laser beams. An effective intensity, instead of the input intensity, is used in the calculation. In other words, the input intensity is multiplied by $[1-\exp(-\bar{\alpha}d)]/(\bar{\alpha}d)$ to correct the influence of the scattering effect on the molecular reorientation angle. And the effective gain is defined by

$$g_{sc} \equiv \frac{I_{Do}}{I_{wkt}} = \frac{I_{wke}J_0^2(\delta_1) + I_{ste}J_1^2(\delta_1)}{I_{wkt}}, \tag{11}$$

where the effective intensities

$$I_{wke} = I_{wk}\{[1-\exp(-\bar{\alpha}d)]/(\bar{\alpha}d)\}, \quad I_{ste} = I_{st}\{[1-\exp(-\bar{\alpha}d)]/(\bar{\alpha}d)\}$$

and I_{wkt} is the transmitted intensity for I_{wk} alone, i.e. $I_{wkt} = I_{wk}\exp(-\bar{\alpha}d)$, $\bar{\alpha}$ is the effective scattering coefficient determined by experimental measurement. The numerical calculation has been done for a planar cell. The physical parameters of 5CB are

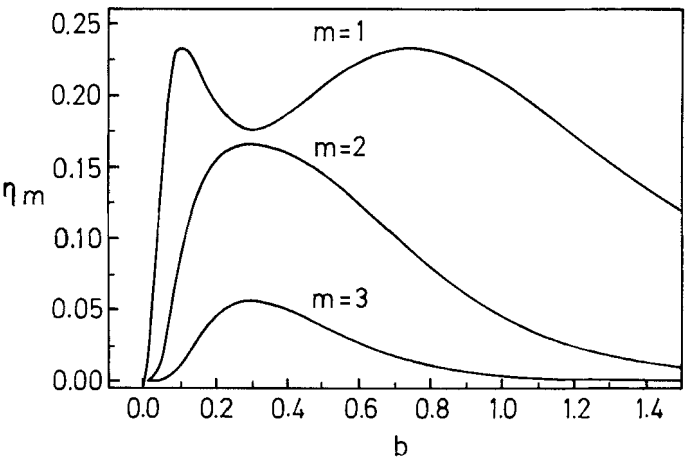

(*a*)

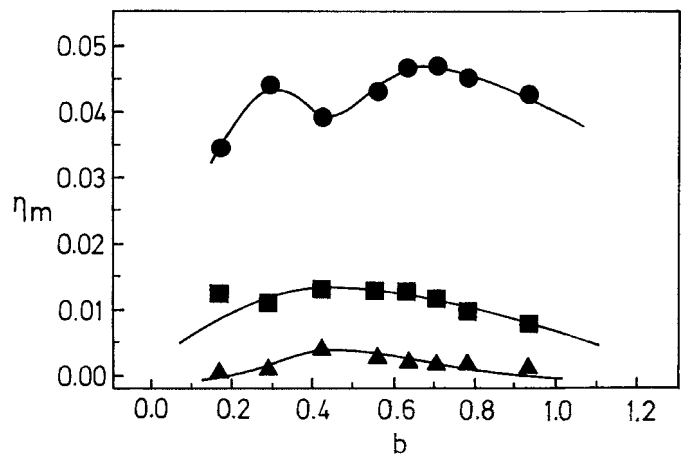

(*b*)

Figure 4. Numerical results (*a*) and experimental results (*b*) of the diffraction efficiency η_m versus the reduced effective field b, for $I_1 = I_2$, shows $\phi_{11} < \delta_{1m} < \phi_{21}$. The solid lines plotted in (*b*) are a guide to the eyes. (*a*) $I_t/I_{th} = 0{\cdot}08$; (*b*) $I_t/I_{th} = 0{\cdot}08$; ●, $m=1$; ■, $m=2$; ▲, $m=3$.

used. These are $n_e = 1{\cdot}75$, $n_o = 1{\cdot}543$, $K_1 = 0{\cdot}51 \times 10^{-6}$ dyne, $K_2 = 0{\cdot}28 \times 10^{-6}$ dyne, $K_3 = 0{\cdot}69 \times 10^{-6}$ dyne and $\Delta\varepsilon = 10{\cdot}9$. Using equations (2), (4), (5), (6) and (11), the effective gains have been calculated for three different I_t/I_{th} values 0·04, 0·08 and 0·12 with fixed beam ratio 40. The results are shown in figure 6 (*a*).

It is obvious, in this region of the total intensity, that the effective gain reaches its maximum g_{sem} at an optimum biased field. And the gain increases as the total intensity increases. The maximum effective gain g_{sem} versus the beam ratio for $I_{st}/I_{th} = 0{\cdot}04$, 0·08, 0·12, 0·16 and 0·2 is plotted in figure 7 (*a*). The maximum gain increases with increasing beam ratio and then saturates as predicted by the small distortion analysis in the theory.

The maximum effective gain obtained at the optimum biased electric field versus the total input intensity is shown in figure 8 (*a*). The maximum effective gain increases monotonically with respect to the total input intensity.

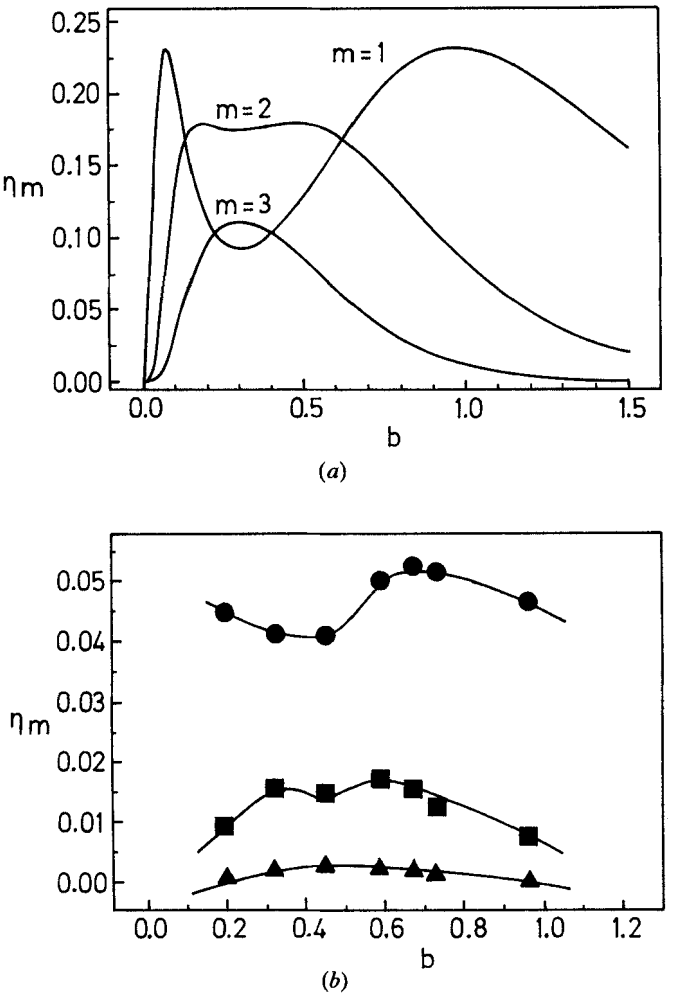

Figure 5. Numerical results (*a*) and experimental results (*b*) of the diffraction efficiency η_m versus the reduced effective field b, for $I_1 = I_2$, shows $\phi_{21} < \delta_{1m} < \phi_{31}$. The solid lines plotted in (*b*) are a guide to the eyes. (*a*) $I_t/I_{th} = 0{\cdot}099$; (*b*) $I_t/I_{th} = 0{\cdot}099$; ●, $m=1$; ■, $m=2$; ▲, $m=3$.

4. Experimental results

The experimental method is essentially the same as described in our previous reports [7], except that we need more detectors to measure more than one diffraction beam simultaneously. The Ar^+ laser light source and 1 KHz biased electric field were used in the experiment. The experimental results for a homeotropically aligned MBBA cell are shown in figures 3(*b*), 4(*b*) and 5(*b*) to compare with the corresponding numerical results in figures 3(*a*), 4(*a*) and 5(*a*), respectively. To make the high order diffraction detectable, high intensity beams have to be used. This makes the measurement of diffraction intensity difficult due to the diffraction ring effect [9]. However, the general behaviour of the diffraction efficiency is reasonable compared to the numerical results. The low diffraction efficiency is due to scattering loss.

For weak beam amplification, a planar cell of 5CB was used. The scattering loss is represented by an effective scattering coefficient $\bar{\alpha}$. Allowing one beam to pass through the sample alone, the intensities I and I' before and after the cell, respectively, can be

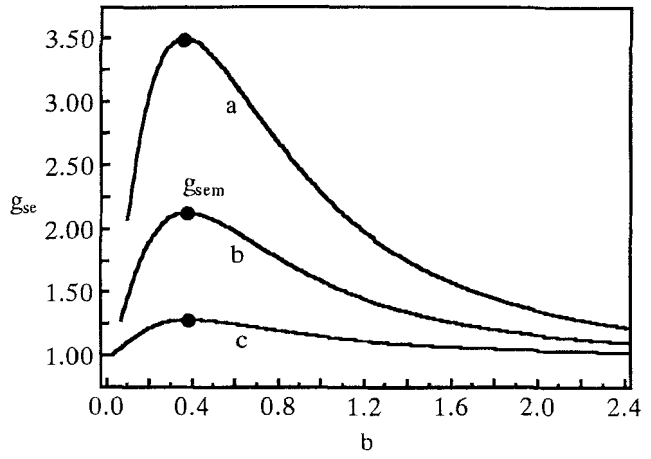

(*a*)

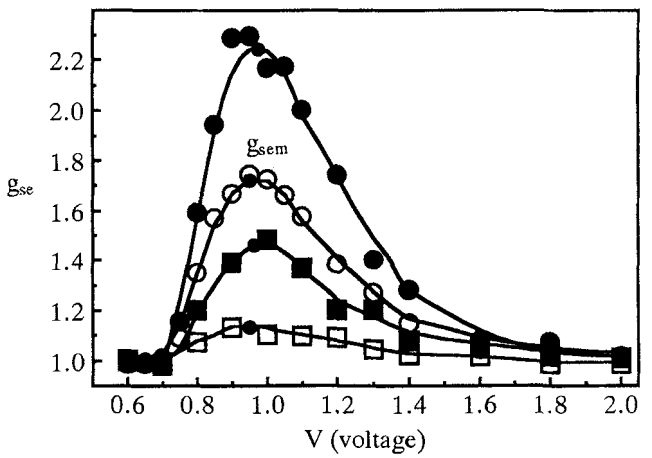

(*b*)

Figure 6. (*a*) Numerical results of the effective gain g_{se} versus the reduced effective field b for $I_{st}/I_{wk}=40$. I_t/I_{th}: *a*, 0·12; *b*, 0·08; *c*, 0·04. $d=75$ μm, $\Lambda=100$ μm. (*b*) Experimental results of the effective gain g_{se} versus the biased voltage V for $I_{st}/I_{wk}=40$. The solid lines are a guide to the eyes. I_t: ●, 70·7 W cm^{-2}; ○, 43·7 W cm^{-2}; ■, 29·3 W cm^{-2}; □, 15·1 W cm^{-2}. $d=75$ μm, $\Lambda\cong 95$ μm.

measured. Then the relation $I'=I\exp(-\bar{\alpha}d)$ is used to determine $\bar{\alpha}$. The experimental results corresponding to the numerical calculation are shown in figures 6 (*b*), 7 (*b*) and 8 (*b*). The effective gain versus biased electric field is shown in figure 6 (*b*) for four different total input intensities. Indeed, there is a maximum effective gain at an optimal biased electric field and the maximal effective gain g_{sem} increases as the total intensity increases. However, for a fixed total input intensity, the increment of the beam ratio will increase the maximum gain only to a saturating value as shown in figure 7 (*b*). In figure 8 (*b*) we can see that the maximum effective gain increases monotonically when the total intensity is increased.

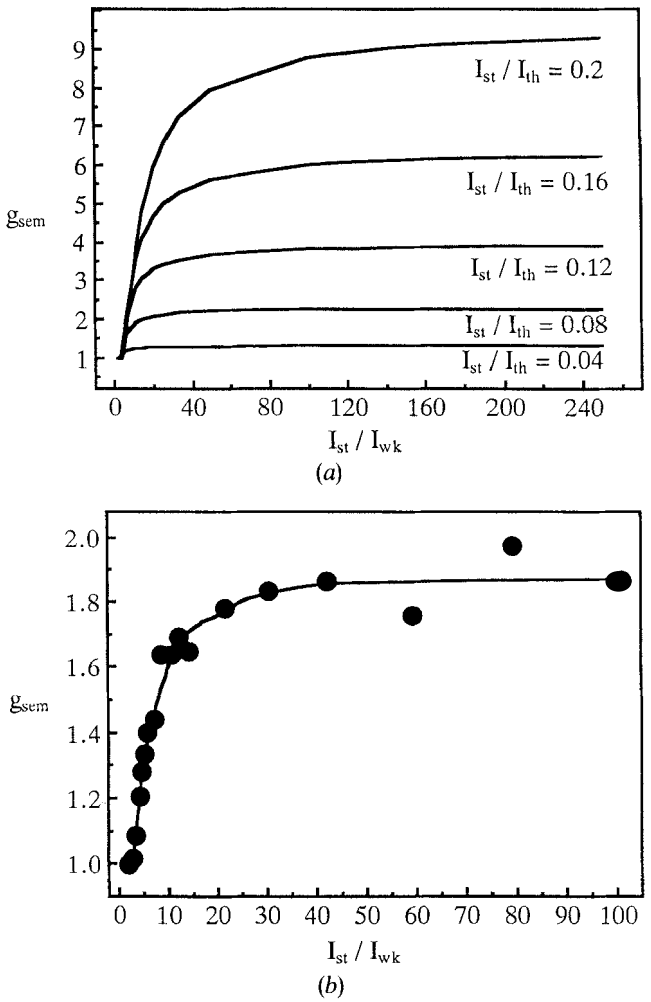

Figure 7. Numerical results (*a*) and experimental results (*b*) of the maximum effective gain g_{sem} versus the beam ratio I_{st}/I_{wk}. The solid line plotted in (*b*) is a guide to the eyes. (*a*) $\Lambda = 100\,\mu m$, $d = 75\,\mu m$, (*b*) $\Lambda \cong 95\,\mu m$, $d = 75\,\mu m$, $I_{st} = 56{\cdot}65\ W\,cm^{-2}$.

5. Discussion and conclusions

In this paper we have extended our previous study on an electric field biased nematic film to include both homeotropic and planar cells. For a homeotropically aligned cell with nematics of negative dielectric anisotropy, the electric field likes to tilt the director away from the unperturbed direction, as do the linearly polarized normally incident laser beams. However, for a planar cell with positive dielectric anisotropy, the electric field also likes to tilt the director but the laser beam does not perturb the director since the polarization of light is in the easy direction. In other words, in this experimental geometry for a known thermotropic nematic liquid crystal which usually has positive optical anisotropy we cannot achieve wave mixing in a planar cell via molecular reorientation without a biased external field, although the intensity has a periodical spatial distribution. The electric field plays a crucial role for wave mixing via molecular reorientational excitation in this geometry.

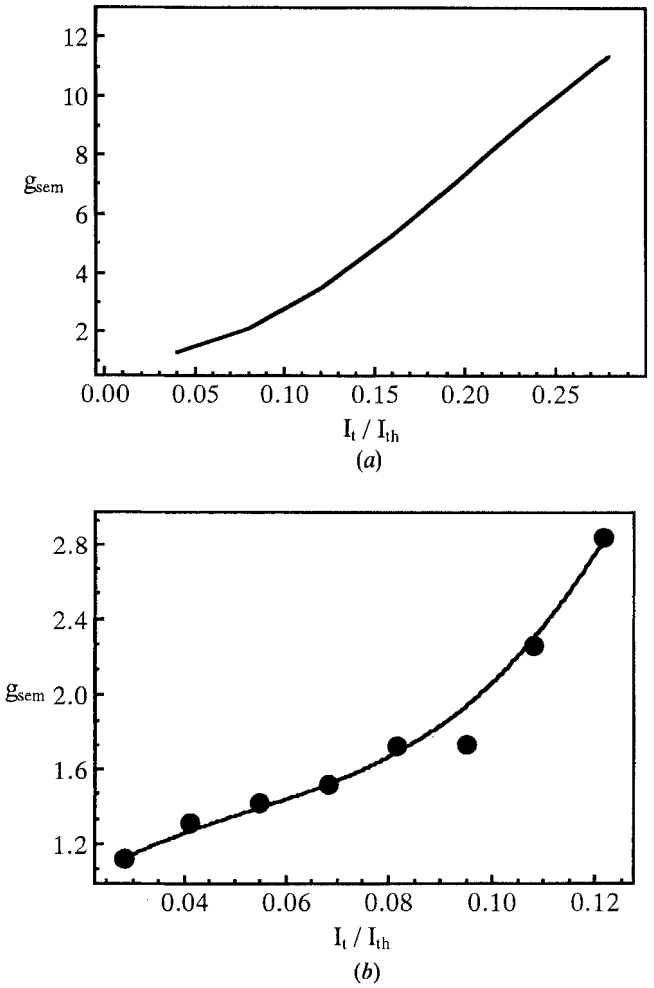

Figure 8. Numerical results (*a*) and experimental results (*b*) of the maximum effective gain g_{sem} versus I_t/I_{th}. The solid line plotted in (*b*) is a guide to the eyes. (*a*) $d=75\,\mu m$, $\Lambda=100\,\mu m$, $I_{st}/I_{wk}=40$, (*b*) $d=75\,\mu m$, $\Lambda\cong 95\,\mu m$, $I_{st}/I_{wk}=40$.

It has to be emphasized that although the nematic liquid crystal has been usually treated as a Kerr medium, the Kerr coefficient n_2 is not a constant, it depends not only on the intrinsic properties of the NLC but also on the experimental geometry. For material excitation of the molecular reorientation type, n_2 can be zero. One example is our planar cell experiment with negative reduced effective field. A crucial factor for inducing molecular reorientation, and thereby wave mixing, is the orientation of the polarization of the input beams with respect to the unperturbed direction of the NLC director.

The diffraction ring effect generally accompanies the wave mixing produced by laser beams in liquid crystals. With an electric field biased cell, the phase grating via molecular reorientation can be easily achieved for low laser intensity. However, for high order diffraction to be detectable, high laser intensity has to be used and the diffraction ring is observable. Therefore the experiment for high order diffraction is difficult. Nevertheless, the general behaviour of the diffraction beams described in the

theory is verified by the experiment using a homeotropically aligned MBBA cell. The behaviour of the transmission beam is shown by weak beam amplification through a planar cell of 5CB. The fraction of intensity loss is not significantly dependent on the input laser intensity and is less than one half in our experiment.

In summary, continuum theory can be successfully utilized to calculate the molecular reorientation angle for the wave mixing process in a nematic liquid crystal cell. The Kerr coefficient is directly related to the characteristic of the special configuration of the induced molecular reorientation. The general formulae have been derived for two experimental configurations namely, homeotropic and planar films with polarization of input beams perpendicular and parallel, respectively, to the easy direction. The concept of a thin film grating is used to describe the diffraction efficiency. The behaviour of the diffraction beams with respect to the reduced effective field is characterized by the properties of the Bessel function and the amplitude of the phase modulation. The biased field plays an important role in this wave mixing process. The existence of multi-peaks of diffraction efficiency is determined by the maximum amplitude of the modulation phase. Weak beam amplification is possible via the molecular reorientational excitation.

This research was supported in part by the Chinese National Science Council under Contract No. NSC-81-0417-M-009-01.

References

[1] SHEN, Y. R., 1986, *I.E.E.E. Jl quant. Electron.*, **22,** 1196.
[2] LIU, T. H., and KHOO, I. C., 1987, *I.E.E.E. Jl quant. Electron.*, **23,** 2020.
[3] HERMAN, R. M., and SERNIKO, R. J., 1979, *Phys. Rev.* A, **19,** 1975.
[4] CHEN, S. H., and KUO, C. L., 1991, *Molec. Crystals liq. Crystals*, **207,** 131.
[5] CHEN, S. H., and KUO, C. L., 1989, *Appl. Phys. Lett.*, **55,** 1820.
[6] KUO, C. L., and CHEN, S. H., 1990, *Optics Lett.*, **15,** 610.
[7] KUO, C. L., and CHEN, S. H., 1990, *J. appl. Phys.*, **68,** 4413.
[8] KUO, C. L., CHEN, S. H., and WEI, J. G., 1993, *Optic Lett.* (to be published).
[9] DURBIN, S. D., ARAKELIAN, S. M., and SHEN, Y. R., 1981, *Optics Lett.*, **6,** 411.